Int. J. Multiphase Flow Vol. 16, No. 3, pp. 545–559, 1990
Printed in Great Britain.

0301-9322/90 $3.00 + 0.00

EXTENSIONAL FLOW OF POLYDISPERSE FIBRE SUSPENSIONS IN FREE-FALLING LIQUID JETS

J. F. T. PITTMAN and J. BAYRAM
Department of Chemical Engineering, University College of Swansea, University of Wales, Swansea SA2 8PP, Wales

(*Received* 23 *May* 1989; *in revised form* 23 *January* 1990)

Abstract—Experimental results for axial velocity profiles in free-falling jets of a Newtonian liquid were in close agreement with numerical solutions of a mathematical model of the jet. The model was fitted successfully to experimental results for jets of fibre suspension by adjustment of an effective suspension extensional viscosity. The occurrence of polydispersity in fibre suspensions is discussed, and theoretical results for viscosity of aligned fibre suspensions in uniaxial extension are re-written to take into account distributions of fibre length and diameter. These distributions were determined experimentally, and predictions based upon them compared with experimental results. It is found that, over a 20-fold range of concentration (0.04–0.9 vol%) and a 6-fold change in fibre aspect ratio (0.5 and 3 mm × 10 μm), experimental values closely follow the form of concentration dependence exhibited by the close particles theory, but lie 15% below its predictions. They also lie 50% below the values given by an interpolation formula suggested for use in the intermediate concentration range occupied by the experiments. Irregularity in the jet flow was encountered which increased in severity with concentration and ratio of fibre length to jet diameter. This is believed to be due to fibre clumping resulting from the impossibility of complete fibre dispersion and alignment as concentration approaches 10% of the limiting value for a random three-dimensional aggregation of rigid rods. This conclusion means that it may, in practice, be very difficult to achieve the conditions upon which the "close particles" theory is based.

Key Words: extensional flow, extensional viscosity, fibre suspensions, liquid jets, polydisperse suspensions, fibre dispersion

INTRODUCTION

The present work formed part of a study of processes for production of felts of aligned short fibre, known as "pre-pregs", as precursors in the fabrication of articles from fibre-reinforced plastic. For the high performance composites which are of interest, quite precise parallel alignment of fibres is required, so that close packing and high volume fractions can be obtained. This alignment is brought about using extensional flows of fibre suspensions, and in previous papers (Harris & Pittmann 1976; Salariya & Pittman 1980) we have studied a process in which a free-falling sheet of suspension is deposited on to a moving filter surface, where the suspending liquid is rapidly removed as the felt of aligned fibres builds up. In an alternative arrangement, a jet of circular cross-section falls onto the filter surface, and it is behaviour of this free-falling jet of fibre suspension which is the subject of the present work. Specifically we are interested in predicting its axial velocity profile, which requires knowledge of the viscosity of the suspension in uniaxial extension and the substitution of this into a fluid mechanical model of the jet. The stability of the jet is also of practical importance.

In addition to their relevance to the process mentioned above, these topics are of more general interest. The extensional viscosity of suspensions of slender, rod-like particles has received a certain amount of attention, both because of its intrinsic fluid mechanical interest and because the suspensions can in some cases be considered as models of polymer solutions. The mathematical modelling of liquid jets is of importance in a number of applications, including experiments to determine extensional viscosities, and jet instability can cause difficulties in these experiments.

In the following sections we first briefly review previous theoretical and experimental work on the viscosity of aligned fibre suspensions in uni-axial extension. A mathematical model of a jet is then solved numerically and its predictions compared with experimental measurements on a jet of a fibre-free Newtonian liquid. Measurements on jets of fibre suspensions are then reported and the mathematical model is fitted to the results to obtain extensional viscosities. Jet irregularities are

observed, and some suggestions are offered as to their origin. The composite production process which has been referred to requires the use of lower viscosity suspending liquids than have generally been used in previous work on extensional viscosities of fibre suspensions, and this seems to decrease jet stability. In addition, limits are set on the suspension concentrations which may be used, to avoid incomplete dispersion of fibres and loss of the desired alignment pattern. These limits put the present experiments in an intermediate range of concentrations, between those for which successful theoretical predictions of extensional viscosity exist. The present results are therefore of interest in providing an indication of suspension behaviour in this range, which is of some practical importance.

PREVIOUS WORK ON ALIGNED FIBRE SUSPENSIONS IN EXTENSION FLOW

Theoretical results for extensional viscosity

In a uniaxial extensional flow of fibre suspension, and where it is assumed that fibre axes are parallel to the principal axis of fluid strain, the bulk stress in the suspension can be expressed (Batchelor 1971) as

$$\sigma_{ij} = -P\delta_{ij} + 2\mu\, e_{ij} + 3(p_i p_j - \tfrac{1}{3}\delta_{ij})\mu e_{11}\,\lambda, \qquad [1]$$

where the last term is the deviatoric stress component due to the suspended particles. Here **p** is a unit vector along the particle axis and μ is the Newtonian viscosity of the suspending liquid. For the case of a dilute suspension of particles λ is given by

$$\lambda_{\text{dil}} = \frac{4\pi}{9}\sum_p l_p^3 \epsilon_p Q(\epsilon_p) \qquad [2a]$$

where the summation is over all particles, p, in unit volume. For uniform particles of length $2l$ and radius R,

$$\lambda_{\text{dil}} = \tfrac{2}{9} C \frac{l^2}{R^2}\epsilon Q(\epsilon), \qquad [2b]$$

where

$$\epsilon = \frac{1}{\ln\dfrac{2l}{R}}. \qquad [3]$$

$Q(\epsilon)$ is obtained from slender body theory as

$$Q(\epsilon) = \frac{1 + 0.640\epsilon}{1 - \frac{3}{2}\epsilon} + 1.659\,\epsilon^2 + O(\epsilon^3). \qquad [4]$$

The criterion for diluteness of a suspension with n particles per unit volume is

$$nl^3\epsilon \ll 1. \qquad [5]$$

For more concentrated suspensions, where the average interparticle spacing is h, a cell model gave the following:

$$\lambda_{\text{cl}} = \frac{4\pi}{9}\sum_p \frac{l_p^3}{\ln\left(\dfrac{h}{R}\right)}; \qquad [6a]$$

or, for a suspension of identical particles,

$$\lambda_{\text{cl}} = \frac{2}{9} C \frac{l^2}{R^2}\frac{1}{\ln\left(\dfrac{h}{R}\right)} \qquad [6b]$$

and

$$h = (2nl)^{-\frac{1}{2}}.$$

Validity of equations [6] requires

$$R \ll h \ll l \qquad [7]$$

and the relative error is expected to be of order $[\ln(h/R)]^{-1}$.

For intermediate conditions, Batchelor (1971) proposed

$$\lambda_{\text{int}} = \frac{4\pi}{9} \sum \frac{l^3}{\ln\left(\frac{2l}{R}\right) - \ln\left(\frac{h+2l}{h}\right) - 1.5}, \qquad [8]$$

which reduces to the spheroidal particle version of [2a] when $h \gg l$, and to [6a] as $h/l \to 0$ and $R/h \to 0$. The assumption of parallel particles restricts the result to the case $l \ll r$, where r is the radial coordinate of the particle centre referred to the origin of the sink (or source) flow.

The theory has been extended by James & Saringer (1980) to take account of the convergence of streamlines in a spherical sink, though still with the use of batchelor's one-dimensional solution for the velocity field around the particle. A more substantial extension has been undertaken by Goddard (1976, 1978) to take account of non-Newtonian behaviour of the suspending medium.

Modelling of fibre suspensions in more general flow fields has recently advanced significantly (Dinh & Armstrong, 1984; Lipscomb *et al.* 1988). Extensional components of the flow, however, are often dominant, because resistance to deformation is relatively very high there. Slender particles tend rapidly to align along streamlines, so the extensional vicosity of aligned fibre suspension remains a topic of considerable interest.

Experimental

There have been a number of experimental tests of the Batchelor (1971) theory. Mewis & Metzner (1974) determined extensional viscosities by measuring thrust on a spinnaret. Suspensions of glass fibre in a liquid with Newtonian viscosity 283 P were used. Parameter values and results are summarized in table 1. In experiments 1–4, experimental values differ from the close particles theory by −9.7 to 18.2%. There seems to be no correlation between these departures and values of the parameters h/l and R/h, which determine the applicability of the theory. These parameters have similar values in experiment 5, but the experimental result is now 29.4% low. We wonder whether this is due to breakage and length reduction of the long (12 mm) fibres used in this experiment. The following experimental problems were noted by Mewis & Metzner (1974). Difficulty in dispersing fibres into suspension limited concentrations to those shown. "Draw-resonance" occurred, leading to fluctuations in thrust and jet diameter; this was more pronounced when using longer fibres and higher concentrations. Interparticle spacing was in some cases quite large compared with the jet diameter. Thus, a proportion of the jet cross-section adjacent to the surface could be considered free of fibres, with a resulting reduction in stress levels. The "fibre-free" region varied from 7 to 13% of the cross-section at 0.1% concentration and from 21 to 30% at 1% concentration. No corrections were applied to measured stresses for these effects. Fibres within

Table 1. Summary of experimental work on the extensional viscosity of aligned fibre suspensions

Reference	$2l$ (mm)	C (vol%)	$\frac{l}{R}$	$\frac{h}{l}$	$\frac{R}{h}$	λ_{exp}	λ_{cl} [8]	$(\lambda - \lambda_{\text{cl}})/\lambda_{\text{cl}}$ (%)
Mewis & Metzner (1974)	3.10	0.930	282	0.074	0.048	51	56.45	−9.7
	6.375	0.099	586	0.108	0.016	17.5	18.74	−6.6
	6.375	0.287	586	0.064	0.027	74	62.59	+18.2
	6.375	0.890	586	0.036	0.047	260	231.54	+12.3
	12.065	0.096	1259	0.052	0.016	59	83.56	−29.4
Weinberger (1970)	0.2	1.3	57	0.27	0.064	9–10	3.5	
Kizior & Seyer (1974)	1.27	0.090	85	0.987	0.024	All	0.46	
	1.27	0.185	85	0.688	0.034	$\sim\lambda_{\text{cl}}+2$	0.80	
	1.27	0.278	85	0.562	0.042		1.27	
	2.54	0.093	170	0.485	0.024		1.47	
	2.54	0.185	170	0.344	0.034		3.20	
	3.81	0.093	255	0.323	0.024		3.31	
	5.08	0.093	340	0.243	0.024		5.88	

each sample were considered effectively identical, and no measurements of fibre dimensions were reported. A technique similar to that of Mewis & Metzner (1974) had earlier been used by Weinberger (1970) and Weinberger & Goddard (1974) in measurements on suspensions of glass fibre in silicone oil (1025 P) and Indopol (205 P). The parameters shown in table 1 indicate that these experiments are outside the range of validity of the close particles formula, as noted by Batchelor (1971). However, the experimental result of about 9 agrees quite well with the value of 8.6 from the formula proposed by Batchelor for interpolation between the dilute and close particles cases.

Kizior & Seyer (1974) used a different technique in which the thrust of a jet issuing from a sharp-edged orifice was measured. Interpretation of the results relies upon knowledge of the flow kinematics upstream of the orifice. Viscose rayon fibre was used in sugar solutions of 1.8 and 0.52 P. From the information provided one can derive the parameters shown in table 1. Values of h/l are rather large for the close particles formula to apply, and experimental results were found to equal approximately $\lambda_{cl} + 2$ over the range studied; i.e. values seemed not to tend to zero as λ_{cl} becomes small. It was suggested that the discrepancy resulted from an incorrect assumption about flow upstream of the orifice.

Chan *et al.* (1978) have presented data on the extensional viscosity of a high density polyethylene melt loaded with 9 and 22 vol% of glass fibre. Goddard (1978a, b) found that agreement of this data with the Batchelor–Goddard theory was not good, and this led White & Czarnecki (1980) to reconsider the experiments. They concluded that fibre lengths were significantly less than the nominal values which had previously been assumed, due to breakage during processing. Length distributions were obtained for processed materials and a number of lengths means evaluated, namely

$$\bar{L}_n = \frac{\Sigma N_i L_i}{\Sigma N_i}, \quad \bar{L}_w = \frac{\Sigma N_i L_i^2}{\Sigma N_i L_i}, \quad \bar{L}_z = \frac{\Sigma N_i L_i^3}{\Sigma N_i L_i^2}, \qquad [9]$$

where N_i is the number of fibres in the sample of length L_i. They suggest, without explanation, that l^2 in [6b] should be replaced by $\frac{1}{4}\bar{L}_z\bar{L}_w$. However, it was found that best agreement with theory was obtained using $\frac{1}{4}(\bar{L}_w)^2$.

In summarizing the experimental work one can say that the most conclusive test of theory is the comparison of the close particles formula with the results of Mewis & Metzner (1974). Agreement is generally satisfactory, but given the strong dependence of λ on the particle aspect ratio it is clearly necessary to recognize that suspensions are likely to be polydisperse, and to determine fibre dimensions in the suspensions actually used. In a number of other works the experimental conditions lie between the conditions under which either the close or dilute suspension results are expected to hold. In this category, the results of Kizior & Seyer (1974) are rather inconclusive, and only a single point is available from Weinberger (1970). As these intermediate conditions are of some practical importance, the present work aims to provide some data in this region.

POLYDISPERSE FIBRE SUSPENSIONS

Occurrence of polydispersity

Our experience has been that glass, carbon fibre etc. chopped to a nominal length, generally shows a significant spread of lengths. In addition, a less significant variation in diameters occurs, due to fluctuations in the manufacturing process. The more important source of polydispersity, though, is the reduction of fibre length due to breakage during preparation of suspensions or other processing, and it is appropriate to discuss this a little further. In view of the high ultimate tensile strength of most fibres it is very unlikely that they would be broken by tensile stresses induced by an extensional flow parallel to the fibre axis. However, in other situations, fibres will rotate, and may bend as they do so; it is the stresses induced by bending which are likely to cause breakage. Salinas & Pittman (1981) studied the bending and breaking of fibres as they rotate in a simple shear flow. From thin-rod theory the dimensionless critical radius of curvature at which a fibre breaks is equal to the ratio of its Young's modulus and ultimate tensile strength:

$$\left(\frac{R_c}{R}\right)_{break} = \frac{E}{T}. \qquad [10]$$

The minimum dimensionless curvature of a fibre as it rotates in the simple shear, with shear rate $\dot{\gamma}$, can be expressed as a function of a dimensionless stiffness number (Salinas 1981) s^*,

$$\left(\frac{R_c}{R}\right)_{\min} = f(s^*), \quad s^* = \frac{E}{\dot{\gamma}\mu(l/R)^4}. \qquad [11]$$

Thus, for a given material (E/T fixed), a critical value s^*_{break} is defined, such that if $s^* < s^*_{\text{break}}$, then breakage occurs. This in turn implies that at critical breaking conditions the fluid shear stress is inversely proportional to the fourth power of the fibre aspect ratio,

$$(\dot{\gamma}\mu)_{\text{break}} \propto \left(\frac{R}{l}\right)^4_{\text{break}}. \qquad [12]$$

The difficulty of forming or processing a suspension without breaking fibres is thus seen to increase very rapidly with the fibre aspect ratio.

During processing, fibres which pass through high shear stress regions will break, but processing will not usually continue long enough for all fibres to pass through these regions, and a polydisperse suspension will result.

Theoretical results for extensional viscosity of polydisperse aligned fibre suspensions

Batchelor's (1971) results for stresses in uniaxial extensional flow of aligned fibre suspensions are easily re-written to take account of a distribution of fibre lengths and radii. Introduce differential distribution functions $f(l)$ and $g(R)$ for length and radius, such that the fraction of fibres with half length l', $l \leqslant l' \leqslant l + \delta l$, is $f(l')\delta l$ etc. and

$$\int_0^\infty f(l)\,\mathrm{d}l = \int_0^\infty g(R)\,\mathrm{d}R = 1. \qquad [13]$$

When polydispersity has occurred through fibre breakage some correlation may exist between l and R, since critical breaking conditions depend on the aspect ratio. However, in practice, this would be difficult to quantify and we shall assume independent distribution functions as given above.

For the dilute suspension case, replace the summation in [2a] using the distribution functions, and introduce n, the number of particles per unit volume:

$$\lambda_{\text{dil}} = \frac{4\pi}{9} n \int_0^\infty \int_0^\infty l^3 \epsilon Q(\epsilon) f(l) g(R)\,\mathrm{d}l\,\mathrm{d}R. \qquad [14]$$

The volumetric concentration is expressed as

$$C = 2\pi n \int_0^\infty l f(l)\,\mathrm{d}l \int_0^\infty R^2 g(R)\,\mathrm{d}R \qquad [15]$$

and substituting for n from [15], into [14]:

$$\lambda_{\text{dil}} = \tfrac{2}{9} C \frac{\displaystyle\int_0^\infty \int_0^\infty l^3 \epsilon Q(\epsilon) f(l) g(R)\,\mathrm{d}l\,\mathrm{d}R}{\displaystyle\int_0^\infty l f(l)\,\mathrm{d}l \int_0^\infty R^2 g(R)\,\mathrm{d}R}. \qquad [16]$$

In practice the distributions will be obtained as histograms rather than continuous functions. Hence, introduce f_p for the fraction of fibres with half length l in the range

$$l_p - \frac{\Delta l}{2} < l < l_p + \frac{\Delta l}{2}, \qquad [17]$$

and g_p for the fraction with radius R in

$$R_q - \frac{\Delta R}{2} < R < R_q + \frac{\Delta R}{2}, \qquad [18]$$

then the ratio of integrals in [16] is evaluated approximately as

$$\frac{\sum_q \sum_p l_p^3 \epsilon_{pq} Q(\epsilon_{pq}) f_p g_q}{\sum_p l_p f_p \sum_q R_q^2 g_q}. \qquad [19]$$

For the close particles case it is first necessary to evaluate the mean interparticle spacing h, for use in the cell model. One would not expect there to be any correlation between the separation of the axes of a pair of fibres and the lengths of those fibres. The mean interparticle spacing is therefore calculated simply on the basis of the total length of all fibres in a unit volume of suspension, as for the uniform fibres case, but now taking into account the length distribution. (It would presumably be possible to make use of a statistical distribution of h values, both for the mono- and polydisperse cases, but given the approximations inherent in the cell model, this does not seem justified). Thus, the length of all particles in a unit volume is

$$n \int_0^\infty 2lf(l)\,\mathrm{d}l \qquad [20]$$

and the average number of particles piercing a unit area perpendicular to the direction of particle alignment is the reciprocal of this quantity. The average interparticle distance is then of order h, where

$$h^2 = \frac{1}{2n \int_0^\infty lf(l)\,\mathrm{d}l}. \qquad [21]$$

Substituting for n from [15],

$$h = \left[\frac{\pi}{C} \int_0^\infty R^2 g(R)\,\mathrm{d}R\right]^{1/2} = \sqrt{\frac{\pi}{C}}\, R_{\text{r.m.s.}}. \qquad [22]$$

Writing h in this form, and introducing the distribution functions to [6a] we obtain, after substitution for n in terms of C,

$$\lambda_{\text{cl}} = \tfrac{2}{9} C \frac{\int_0^\infty \int_0^\infty \dfrac{l^3}{\ln\left(\sqrt{\dfrac{\pi}{C}} \dfrac{R_{\text{r.m.s.}}}{R}\right)} f(l) g(R)\,\mathrm{d}l\,\mathrm{d}R}{\int_0^\infty lf(l)\,\mathrm{d}l \int_0^\infty R^2 g(R)\,\mathrm{d}R}. \qquad [23]$$

In the same way as for [16] the ratio of integrals may be approximated by

$$\frac{\sum_q \sum_p \dfrac{l_p^3}{\ln\left(\dfrac{\pi}{C} \dfrac{R_{\text{r.m.s.}}}{R_q}\right)} f_p g_q}{\sum_p l_p f_p \sum_q R_q^2 g_p}. \qquad [24]$$

For particles of uniform radius, the averaging here corresponds to the use of $\bar{L}_z\, \bar{L}_w$, as proposed by White & Czarnecki (1980).

The interpolation formula, [8], can be re-written as

$$\lambda_{\text{int}} = \tfrac{2}{9} C \frac{\int_0^\infty \int_0^\infty \dfrac{l^3 f(l)\, g(R)\,\mathrm{d}l\,\mathrm{d}R}{\ln\left(\dfrac{2l}{R}\right) - \ln\left(\dfrac{h+2l}{h}\right) - 1.5}}{\int_0^\infty lf(l)\,\mathrm{d}l \int_0^\infty R^2 g(R)\,\mathrm{d}R}, \qquad [25]$$

with the integrals evaluated as

$$\frac{\sum_p \sum_q \dfrac{l_p^3 f_p g_p}{\ln\left(\dfrac{2l_p}{R_q}\right) - \ln\left(\dfrac{h_q + 2l_p}{h_q}\right) - 1.5}}{\sum_p l_p f_p \sum_q R_q^2 g_q} \qquad [26]$$

and h is given by [22].

MATHEMATICAL MODELLING OF THE JET

Equation of motion

Modelling of a jet or spin line has been discussed in detail by Matovitch & Pearson (1969), and the model used here corresponds to their zeroth-order approximation, which is expected to hold well except close to the origin of the jet. The following assumptions are made: isothermal, steady flow of a fluid with constant density, ρ, and surface tension, σ. Referring to a cylindrical polar coordinate system with the z-axis coincident with the jet axis, it is assumed that $v_r = v_\theta = 0$ and $\partial a/\partial z \ll 1$, where a is the jet radius. The resulting non-linear equation for the jet velocity is

$$\rho v_z \frac{\partial v_z}{\partial z} = \rho g + 3\mu_s \left[\frac{\partial^2 v_z}{\partial z^2} - \frac{1}{v_z}\left(\frac{\partial v_z}{\partial z}\right)^2\right] - \frac{\sigma \pi^{\frac{1}{2}}}{2Q^{\frac{1}{2}}} \frac{1}{v_z^{\frac{1}{2}}} \frac{\partial v_z}{\partial z}, \qquad [27a]$$

where for the case of an aligned fibre suspension, it follows from [1] that

$$\mu_s = \mu(1 + \lambda), \qquad [27b]$$

where μ is the carrier liquid viscosity.

A first boundary condition can be defined at a suitable point on the jet axis by

$$z = 0, \quad v_z = V_0, \qquad [28]$$

where V_0 is, in practice, an experimentally determined flow velocity at a convenient level in the jet.

A second condition is provided by noting that at large z, velocity tends to the free-fall value

$$z \to \infty, \quad v_z \to \sqrt{2gz}\,. \qquad [29]$$

Numerical solution

The surface tension term in [25] is not negligible in the present work, so the analytic solution due to Clarke (1986), is not applicable. Equation [27a] was therefore solved numerically using Merson's fourth-order Runge–Kutta method. To obtain convergence of the "shooting" method, it proved necessary to integrate in the negative z-direction with initial condition of the form

$$z = Z, \quad v_z = V_z, \qquad [30]$$

where V_z is an estimated value, together with from [29],

$$z = Z, \quad \frac{\partial v_z}{\partial z} = \sqrt{\frac{g}{2Z}}. \qquad [31]$$

V_z was adjusted iteratively using the secant method to match the experimental value at $z = 0$, according to [28]. The assumption that Z is large enough for the free-fall acceleration to apply sufficiently closely was checked by repeating the solution for different values of Z. This solution procedure was previously used by Salariya (1977) in related work on free-falling liquid sheets.

In practice, velocities at $z = 0$ were of the order of 10 cm s^{-1} and solutions were matched to these values within 10^{-4} cm s^{-1}. Z was chosen as 50 cm; reducing the value to 30 cm altered the computed value at $z = 0$ by $< 3\%$. The integration step size was 0.0125 cm, and this gave results accurate to five significant figures.

EXPERIMENTAL APPARATUS AND PROCEDURE

Apparatus

In the equipment to produce free-falling jets, liquid is transferred at room temperature by a variable-speed peristaltic pump from a 5 l. reservoir, where temperature is measured, via a damping vessel to a vertical glass tube which is sufficiently long (50 cm) to eliminate swirling and establish laminar, parallel flow. At its lower end the tube tapers gradually to the orifice, which is ground precisely circular. Tubes with orifices of 2, 4 and 8 mm nominal dia were constructed. A precisely ground tool steel rod of 3.57 mm dia is mounted parallel to the jet axis, and is scribed at 1 cm intervals to provide a vertical scale.

Preparation of solutions and suspensions

Aqueous solutions of D-glucose were prepared, and their viscosity, surface tension and density obtained. Weighed samples of carbon fibre were dispersed to give suspensions of known concentration, assuming the manufacturer's value for the fibre density of 1870 kg m^{-3}. Dispersion was carried out using a disc stirrer at 70 rpm for at least 1 h, followed by at least 5 h de-aeration under vacuum.

Determination of fibre size distributions

Samples for fibre length determinations were prepared by gently squeezing a little suspension between microscope slides and photographing the trapped fibres together with a graticule having divisions of 0.01 cm. The negatives were projected, giving a magnification on to the screen of approx. 90:1 and lengths were measured using dividers and a scale. Typically about 200 measurements were used to generate a length distribution. Fibre diameters were measured using a Quantimet image analyser, at a magnification of 1500.

Jet diameter measurement

The jet and reference rod were photographed simultaneously using flash with back lighting behind a diffuser. Negatives were projected, giving a magnification of approx. 40:1 on the screen. Jet and rod diameters were measured, together with the separation of the vertical scale marks on the rod. According to these measurements, vertical and horizontal scales in the projection pictures differed by $<1\%$.

RESULTS AND DISCUSSION

Axial velocity profiles in jets of fibre-free liquid

Table 2 summarizes conditions for experiments carried out with fibre-free liquid. Figure 1 shows a comparison between computed and experimentally measured axial velocities. The origin for the axial coordinate is taken at about 1 dia below the orifice, to exclude the region where simplying assumptions used in the mathematical model would be expected to fail. Scatter in the experimental values in small and they lie about 2.5% below the computed values. Results for the other five runs showed a similar pattern with experimental values falling up to 4% below computed ones. The reason for this apparently systematic trend is not known; it may be due to a small effect of air drag on the jet, but was not considered important enough to pursue further. Overall the results provide reassurance on the validity of the computed values and the accuracy of the physical property data and experimental velocity measurements.

Table 2. Experiments on fibre-free liquid

Orifice dia (cm)	Liquid viscosity (N s m^{-2})	Velocity at orifice (cm s^{-1})	Liquid density (kg m^{-3})
0.2	0.389	9.42	1323
0.2	0.482	3.38	1327
0.2	0.717	11.16	1335
0.4	2.757	6.96	1337
0.4	3.441	4.50	1372
0.8	1.852	25.85	1359

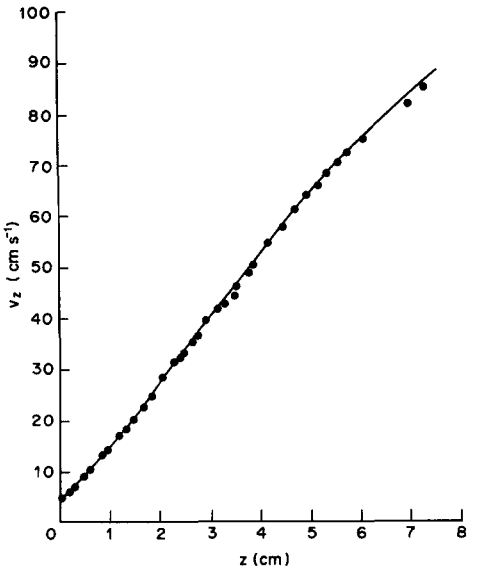

Figure 1. Comparison of computed (——) and experimental (●) axial velocities in a free-falling jet of Newtonian liquid. Orifice dia = 4 mm, liquid viscosity = 34.4 P.

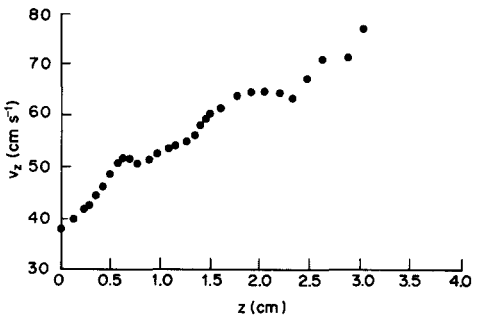

Figure 2. Experimental instantaneous axial velocity profile in a jet of suspension. $2l = 3$ mm nominal, $C = 0.1$ vol%, carrier liquid $\mu = 6.1$ P, orifice dia = 4 mm.

Axial velocity profiles for jets of fibre suspension and jet irregularities

Table 3 shows details of eight experiments carried out with fibre suspensions. It was immediately apparent that in some of these the jets no longer showed the smooth profiles obtained with fibre-free liquid; diameter fluctuations occurred in a roughly periodic way, increasing in amplitude with distance from the orifice. Figure 2 shows the instantaneous axial velocity profile for the worst case, where an extensional viscosity of the suspension could not be determined. Jet irregularities increase with fibre concentration and fibre length, but appear to decrease with orifice diameter (see table 3). The phenomenon seems to be distinct from the "draw resonance" which is familiar in spinning. Irregularities in converging flow towards an orifice have been widely observed in fibre-loaded thermoplastic melts, thermoset resins and other viscous liquids containing fibres. Gibson (1985) and Murty & Modlen (1977) described fibre jamming at the orifice and Gibson gives an expression for a critical concentration based on simple geometrical considerations. Crowson & Folkes (1980) noted pressure fluctuations in capillary rheometry of fibre-loaded resins when fibre length exceeded capillary diameter. Akay (1982, 1983) also observed pressure fluctuations which were associated with the converging flow of suspension into the capillary, and were distinct from stick–slip instabilities which can occur within the capillary. It seems that a range of phenomena may be involved in these observations, but an explanation consistent with observations in the present work is based on the fact that dispersion and fibre alignment is more difficult at higher concentrations of long fibres. Incompletely dispersed

Table 3. Experiments on fibre suspensions[a]

$2l$ (mm)	C (%)	D (mm)	μ (P)	$\frac{h}{l}$	$\frac{R}{h}$	ΔA	Jet	λ_{cl}	λ_{exp}
3	0.04	8	7.66	0.21	0.016	0.17	2	1.796	1.48
3	0.05	4	8.87	0.19	0.018	0.27	3	2.302	1.84
3	0.10	4	6.10	0.13	0.025	0.10	4	5.000	—
0.5	0.14	8	12.44	0.19	0.022	0.13	0	0.314	0.35
0.5	0.30	8	12.44	0.29	0.045	0.06	0	0.746	0.50
0.5	0.90	8	13.29	0.22	0.071	0.04	0	2.657	2.36

[a]Key: $2l$ = nominal fibre length; C = suspension volume concentration; D = orifice dia; μ = carrier liquid viscosity; h = interparticle spacing; R = particle radius; ΔA = fraction of the jet cross-section "fibre-free", mean over the jet height; jet = jet quality, 0—smooth, 5—highly irregular; λ_{cl} = theoretical close particles result, [24, 25]; λ_{exp} = experimental results corrected for fibre-free area, using $1/(1-0.5\,\Delta A)$.

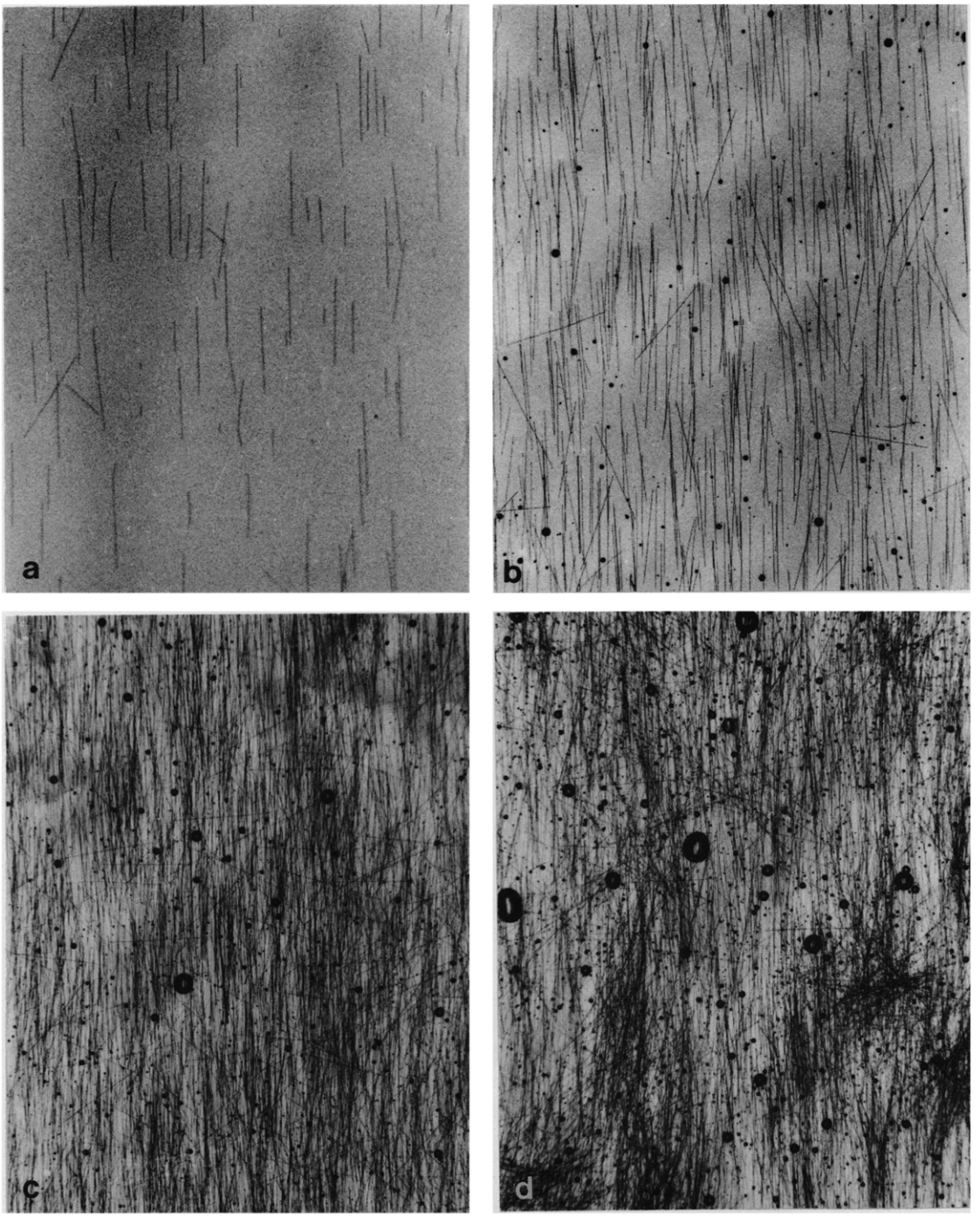

Figure 3. Carbon fibres, 3 mm × 9 μm, in a sheet of suspension falling from the slot at the base of a converging wall channel. (a) $C = 0.02$ vol%, (b) $C = 0.05$ vol%, (c) $C = 0.2$ vol%, (d) $C = 0.4$ vol%.

clumps of fibres may occur leading to periodic partial jamming of the orifice and irregular flow in the jet. Harris & Pittman (1976) found that fibre alignment brought about in a converging flow was impaired at concentrations $\gtrsim 0.2$ vol% for 3 mm × 9 μm fibres, and 1 vol% for $\frac{1}{2}$ mm fibres. Figure 3 shows photographs obtained by Harris (1972) of 3 mm fibres in the free surface liquid sheet falling from the base of an alignment channel. At 0.2 vol% the fibre distribution is patchy, while at 0.4 vol% clumping is clearly evident. Whilst the use of dispersing agents improved the suspension quality a little, a limit seemed to be set by purely geometrical factors. Evans & Gibson

(1988) have shown that the maximum concentration attainable in three-dimensional random aggregations of rod-like particles is given by

$$C_{max} = k\frac{R}{l}, \qquad k \approx 5. \qquad [32]$$

The limiting concentrations found by Harris & Pittman (1976) both correspond to about 0.07 C_{max}, lending support to the idea that they involve similar degrees of fibre–fibre interaction. Folgar & Tucker (1984) found significant fibre–fibre interactions in cylindrical Couette flow at concentrations between 0.1 C_{max} and 0.5 C_{max}. Steady-state orientation distributions were apparent, with the direction of principal alignment offset from the streamline direction, in constrast to dilute suspension theory which predicts periodic variation of the orientation distribution. It is clear that in this concentration region fibre alignment is not predicted well, assuming unhindered rotation. The worst jet irregularities occurred in the present work with a 0.1 vol% suspension of 3 mm fibres; i.e. at half the limiting concentration mentioned above. This is to be contrasted with the smooth jets obtained with suspensions of $\frac{1}{2}$ mm fibres at 0.9 vol%—approximately equal to the limiting concentration. The explanation may lie in the relationship between fibre length and orifice diameter—a rather poorly dispersed suspension of 3 mm fibres being more likely to cause incipient jamming of the 4 mm dia orifice.

Extensional viscosities of suspensions

Effective extensional viscosities were found by iterative adjustment of μ_s in [26] to minimize the standard deviation of experimental velocity values from the computer profile. Precision was about ± 1 P. Figure 4 shows how by the appropriate choice of μ_s, the numerical solution can be fitted to experimental results. The small discrepanacy, noted above, between the computed and experimental velocity profiles for a fibre-free liquid corresponds to possible errors in $\mu_s < 0.5$ P. The effective values of μ_s were then corrected to make some allowance for the "fibre-free" fraction of the jet cross-sectional area, ΔA. By the "fibre-free" region, we mean the outer annulus of the jet cross-section, with radial width equal to the mean interparticle spacing, h. In reality, of course, fibres are present in this region—the term "fibre-free" is based on an idealized view where fibre centres are arranged on a regular grid of side h. Fibres in this surface layer make a smaller contribution to stress levels than fibres deep within the suspension. Following Mewis & Metzner (1974), we assume that they have about half their region of interaction with other fibres intact, and therefore expect their contribution to particle stresses to be reduced by 50%, leading to a reduction over the whole jet cross-section by a factor $(1–0.5\,\Delta A)$. The extensional viscosities are then multiplied by the reciprocal of this factor, to apply a correction for the surface effect.

The resulting values, λ_{exp}, are shown in table 3. ΔA in the reported data are < 0.3, leading to corrections ranging from 2 to 16%. Thus, although there is inevitably some uncertainty in the correction procedure this will not have a large effect on the results.

Figures 5a and 5b show typical experimental fibre length and diameter distributions obtained for a processed suspension. Significant variations about median dimensions are observed, and mean values of length and diameter differ from the nominal fibre dimensions.

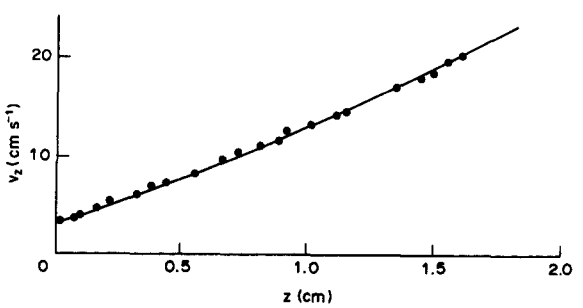

Figure 4. Fit of computed (——) to experimental (●) axial velocities in a jet of suspension, by choice of the effective suspension viscosity. $\mu_s = 44$ P, $2l = 0.5$ mm nominal, $C = 0.9$ vol%, carrier liquid $\mu = 13.3$ P, orifice dia = 8 mm.

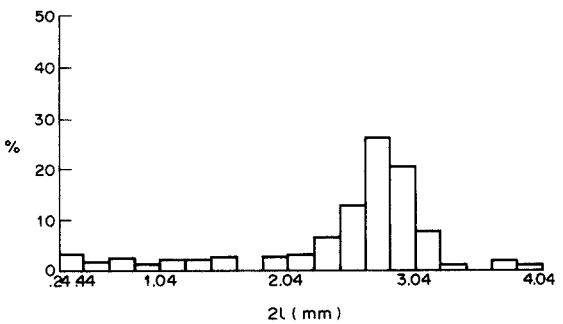

Figure 5a. Length distribution of 3 mm nominal carbon fibres after processes.

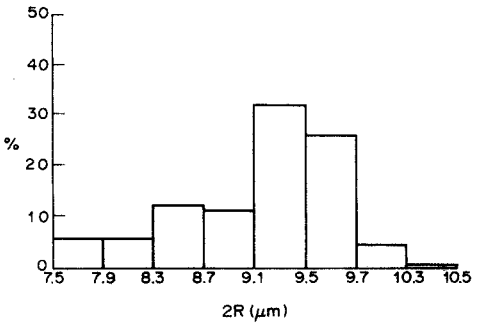

Figure 5b. Diameter distribution of carbon fibres.

According to the theory that has been reviewed, λ should be precisely linear with concentration for dilute suspensions, and nearly so for "close particles". The pooled results for $\frac{1}{2}$ mm and 3 mm fibres are tested for this dependence in figure 6, by plotting λ_{exp} scaled by the square of the aspect ratio, $\bar{l}^2/\bar{R}^2$, based on mean dimensions obtained from distributions such as those shown in figures 5a and 5b. Over a 20-fold change in concentration, a theoretical "close particles" line, based on mean dimensions, provides a good fit to the data, passing through three points and grazing the errors bars of the other two. Note that the error bars here refer to the estimated precision of the fitting process which yields μ_s; additional uncertainties arise from the jet irregularities described above, and this is no doubt the origin of the discrepancies in the two points.

A more rigorous application of the theory, however, takes into account fibre length and diameter distributions, and recalculation of the close particles predictions using [23] and [24] and the experimentally determined distributions gives results some 15% higher. We thus conclude that the previous agreement was fortuitous, and that our results, in fact, lie 15% below the close particles theory predictions. This, nevertheless, quite close agreement may be surprising in view of the fact that experimental conditions correspond to $0.016 \leqslant R/h \leqslant 0.071$ and $0.13 \leqslant h/l \leqslant 0.29$, whereas the theory is expected to hold well only when $R/h \ll 1$ and $h/l \ll 1$. Under experimental conditions the expected relative errors $[\ln(R/h)]^{-1}$ in the stress generated by a fibre are between 25 and 40%.

On the other hand, the criterion for dilute suspensions, $nl^3\epsilon \ll 1$, is clearly not met, with experimental values of $nl^3\epsilon$ lying between 0.1 and 1.0. In this intermediate range, use of the

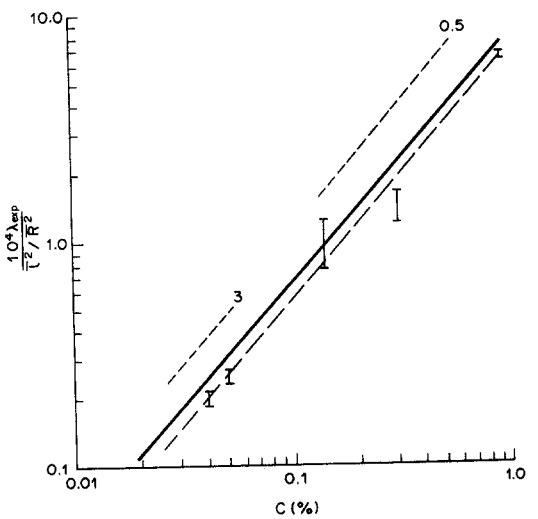

Figure 6. λ Scaled by $\bar{l}^2/\bar{R}^2$ vs concentration. Experimental values λ_{exp} are shown with error bar I; —— close particles theory based on mean fibre dimensions; —— close particles theory based on length and diameter distributions; – – – 0.5, – – – 3, interpolation theory for 0.5 and 3 mm fibres, respectively.

interpolation formula, [8], [25] and [26], has been suggested. The resulting values, based on experimental length and diameter distributions are also shown in figure 6, and are seen to lie substantially above both the experimental results and the close particles theory. Previous results in the intermediate range are due to Kizior & Seyer (1974), whose technique may have been affected by uncertainties; and to Weinberger (1970), who found quite good agreement with the interpolation formula prediction. However, only a single data point was available, and his finding contrasts with the present work, where five points lie on a line about 50% below the interpolation formula values. The reason for this discrepancy remains to be explained.

There remains, though, the fact that our experimental results lie not only below the interpolation formula, but also about 15% below the close particles predictions, taking into account length and diameter distributions. We believe this may be as a result of the incomplete fibre dispersion postulated above, which hinders complete attainment of the parallel fibre alignment upon which the theory is based.

CONCLUSION

Significant flow irregularities were observed in free-falling jets of fibre suspension, the effects being more pronounced at higher concentrations and for larger fibre length to jet orifice diameter ratios. Concentrations approached 10% of a proposed limiting value for random three-dimensional aggregations of rigid rods, and it is suggested that under these conditions complete fibre dispersion cannot be achieved, resulting in fibre clumps which disrupt the jet flow. Evidence for this is provided both by the jet irregularities which have been observed, and by direct observation in the photographs of fibre suspension in figure 3.

Despite this difficulty, results were obtained for extensional viscosity of the suspension, by fitting a mathematical model of jet flow to experimental observations. This technique is experimentally simple, and free from complications, such as "Bourdon tube" effects (Becraft & Metzner 1988), in spinning equipment previously used for extensional viscosity measurement. Extension rates and stresses, however, are not easily varied over a wide range, but this is of less importance in measurements on fibre suspensions in Newtonian media, where extensional viscosity is predicted and found to be independent of extension rate.

Theoretical results due to Batchelor are re-written to take account of fibre length and diameter distributions. The experimental results lie about 15% below the predictions of the close particles theory, taking into account experimentally determined fibre length and diameter distributions. They also lie about 50% below the predictions of an interpolation formula proposed for use in this region.

Taking into account fibre length and diameter distributions alters predictions by 15%, as compared with those based on mean fibre length and diameter. A distribution of fibre lengths arises primarily through fibre breakage, the critical fluid shear stress for fibre breakage varying as the fourth power of the aspect ratio. The relatively small effect of length distributions in the present work is as a result of care taken in forming and handling suspensions, to minimize fibre breakage. Theory predictions based on nominal fibre lengths differed by up to 30% from values based on measured length distributions, illustrating the importance of determining lengths experimentally. The apparently rather low values for extensional viscosity in the present work may result from incomplete fibre dispersion, and for practical purposes we would recommend use of the close particles formula rather than the interpolation, in the region of the experimental conditions, $0.02 < R/h < 0.07$, $0.1 < h/ < 0.3$. A discrepancy between the present results and a single higher value due to Weinberger (1970) remains, however, to be explained.

Finally, we note the importance of fibre–fibre interactions in semi-concentrated suspensions. Present results and references cited indicate that rotation is hindered and the state of parallel fibre alignment, which forms the basis of the close particles theory, may not be fully achieved in practice. This has implications for predictions of extensional viscosities, and for other treatments of fibre suspension rheology which make use of the close particles theory.

REFERENCES

AKAY, G. 1982 Rheology of reinforced thermoplastics and its application to injection-moulding; IV. Transient injection, capillary flow and injection-moulding. *Polym. Engng Sci.* **22,** 1027–1042.

AKAY, G. 1983 Unstable capillary flow of reinforced polymer melts. *J. Non-Newtonian Fluid Mech.* **13,** 309–323.

BATCHELOR, G. K. 1971 The stress generated in a non-dilute suspension of elongated particles by pure straining motion. *J. Fluid Mech.* **46,** 813–829.

BECRAFT, M. L. & METZNER, A. B. 1988 Bourdon tube effects in the fiber spinning apparatus. *Trans. Soc. Rheol.* **32,** 243–270.

CHAN, Y., WHITE, J. L. & OYANAGI, Y. 1978 A fundamental study of the rheological properties of glass-fiber-reinforced polyethylene and polystyrene melts. *J. Rheol.* **22,** 507–524.

CLARKE, N. S. 1986 Two-dimensional flow under gravity in a jet of viscous fluid. *J. Fluid. Mech.* **31,** 481–500.

CROWSON, R. J. & FOLKES, M. L. 1980 Rheology of short glass-fiber-reinforced thermoplastics and its application to injection moulding. II. The effect of material parameters. *Polym. Engng Sci.* **20,** 934–940.

DINH, S. M. & ARMSTRONG, R. C. 1984 A rheological equation of state for semi-concentrated fiber suspensions. *J. Rheol.* **28,** 207–227.

EVANS, K. E. & GIBSON, A. G. 1988 Prediction of the maximum packing fraction achievable in randomly oriented short fibre composites. *Compos. Sci. Technol.* **25,** 149–162.

FOLGAR, F. & TUCKER, C. L. III 1984 Orientation behaviour of fibres in concentrated suspensions *J. Reinforc. Plast. Compos.* **3,** 98–119.

GIBSON, A. G. 1985 Rheology and packing effects in injection moulding of long-fibre reinforced materials. *Plast. Rubb. Process. Applic.* **5,** 95–100.

GODDARD, J. D. 1976 Tensile stress contribution of flow-oriented slender particles in non-Newtonian fluids. *J. Non-Newtonian Fluid Mech.* **1,** 1–17.

GODDARD, J. D. 1978a The stress field of slender particles oriented by a non-Newtonian extensional flow. *J. Fluid Mech.* **78,** 177–206.

GODDARD, J. D. 1978b Tensile behaviour of power-law fluids containing orientated slender fibres. *J. Rheol.* **22,** 615–622.

HARRIS, J. B. 1972 The behavioural of rod-like particles in sheared suspensions. Ph.D. Thesis, Univ. College of Swansea, Wales.

HARRIS, J. B. & PITTMAN, J. F. T. 1976 Alignment of slender rod-like particles in suspension using converging flows. *Trans. Instn chem. Engrs* **54,** 73–83.

JAMES, D. F. & SARINGER, J. H. 1980 Extensional flow of dilute polymer suspensions. *J. Fluid Mech.* **97,** 655–671.

KIZIOR, T. E. & SEYER, F. A. 1974 Axial stress in elongational flow of fibre suspensions. *Trans. Soc. Rheol.* **18,** 271–285.

LIPSCOMB, G. G. II, DENN, M. M., HUR, D. U. & BOGER, D. V. 1988 The flow of fiber suspensions in complex geometries. *J. Non-Newtonian Fluid Mech.* **26,** 297–325.

MATOVICH, M. A. & PEARSON, J. R. A. 1969 Spinning a molten threadline. *Ind. Engng Chem. Fundam.* **8,** 512–520.

MEWIS, J. & METZNER, A. B. 1974 The rheological properties of suspensions of fibres in Newtonian fluids subjected to extensional deformations. *J. Fluid Mech.* **62,** 593–600.

MURTY, K. N. & MODLEN, G. F. 1977 Experimental characterization of the alignment of short fibres during flow. *Polym. Engng Sci.* **17,** 848–853.

SALARIYA, A. K. 1977 The behaviour of rod-like particles in viscous flow. Ph.D. Thesis, Univ. College of Swansea, Wales.

SALARIYA, A. K. & PITTMAN, J. F. T. 1980 Preparation of aligned discontinuous fibre pre-pregs by deposition from suspension. *Polym. Engng Sci.* **20,** 787–797.

SALINAS, A. 1981 Dynamics of flexible fibres in a flowing suspension. Ph.D. Thesis, Univ. College of Swansea, Wales.

SALINAS, A. & PITTMAN, J. F. T. 1981 Bending and breaking fibres in sheared suspensions. *Polym. Engng Sci.* **21,** 23–31.

WEINBERGER, C. B. 1970 Extensional flow behaviour of non-Newtonian fluids. Ph.D. Dissertation, Univ. of Michigan, Ann Arbor.

WEINBERGER, C. B. & GODDARD, J. D. 1974 Extensional flow behaviour of polymer solutions and particle suspensions in a spinning motion. *Int. J. Multiphase Flow* **1**, 465–486.

WHITE, J. L. & CZARNECKI, L. 1980 On papers by Chan, White and Oyanagi and by Goddard on elongational flow behaviour of fiber reinforced polymer melts. *J. Rheol.* **24**, 501–506.